THE ASTROPHYSICAL JOURNAL, 471:203–210, 1996 November 1


# ULTRAVIOLET EXTINCTION BY INTERSTELLAR DUST IN EXTERNAL GALAXIES: M31

LUCIANA BIANCHI[1,2,3]
Space Telescope Science Institute, 3700 San Martin Drive, Baltimore, MD 21218
GEOFFREY C. CLAYTON[1]
Department of Physics and Astronomy, Louisiana State University, Baton Rouge, LA 70803
RALPH C. BOHLIN[1]
Space Telescope Science Institute, 3700 San Martin Drive, Baltimore, MD 21218
J. B. HUTCHINGS[1]
Dominion Astrophysical Observatory, 5071 W. Saanich Road, Victoria, B.C., Canada, V8X 4M6
AND
PHILIP MASSEY[1]
Kitt Peak National Observatory, National Optical Astronomy Observatories,[4] P.O. Box 26732, Tucson, AZ 85726-6732
*Received 1996 March 18; accepted 1996 May 31*

## ABSTRACT

*Hubble Space Telescope* (*HST*) Faint Object Spectrograph (FOS) spectra of stars in OB associations of M31 are used to derive the UV extinction by interstellar dust in M31 by three different methods: (1) comparing spectra of M31 star pairs, (2) comparing spectra of M31 stars to those of Galactic standard stars, and (3) comparing M31 star spectra to atmosphere models. The derived intrinsic M31 extinction curve has an overall wavelength dependence very similar to that of the average Galactic extinction curve but possibly has a weaker 2175 Å bump, however, with a significance of only 1 $\sigma$. This result is different from the LMC (30 Dor)–like curves published earlier, which contained both intrinsic M31 extinction and "foreground" extinction, and were based either on low-signal *IUE* spectra, or on FOS data affected by inaccuracy in the preliminary flux calibration, and were not computed with the pair method used in this work.

In this work, the foreground extinction component from the Galactic halo is also investigated. The foreground curve is consistent with the standard curve. While there is a slight indication for a steeper foreground curve than the standard one, the difference is not significant considering the data uncertainties.

*Subject headings:* dust, extinction — galaxies: individual (M31) — galaxies: ISM — ultraviolet: galaxies

## 1. INTRODUCTION

Understanding interstellar dust and its role in the universe is very important. Virtually all observations of astrophysical objects and their physical processes are affected by the presence of dust either within the system being studied and/or along its line of sight. With a small sample of stars, Bless & Savage (1972) first noted an apparent relationship between low FUV extinction and large $R_V$, the ratio of total-to-selective extinction. This observed correlation suggested that an average Galactic extinction law, $A(\lambda)/A(V)$, depending on only one parameter $R_V$ [$=A(V)/E_{B-V}$], may be applicable to a wide range of interstellar dust environments (Cardelli, Clayton, & Mathis 1989, hereafter CCM; Cardelli & Clayton 1991; Mathis & Cardelli 1992), including lines of sight through diffuse dust, dark cloud dust, and dust associated with star formation. The existence of such a law, valid over the UV wavelength range 3.5–0.125 $\mu$m, would require that the environmental processes that modify the grains are efficient and affect all grains. When changes in the grain size distribution, which are reflected in the FUV extinction, occur as a result of coagulation, the entire size distribution apparently varies in a systematic way. Thus, for instance, the $\sigma$ Sco- and $\zeta$ Oph-type sight lines can be characterized as the extremes of a continuum range of $R_V$ values from large to small (Clayton & Hanson 1993).

While there is some tendency for dust in dark clouds to have higher values of $R_V$ than diffuse sight lines, dark cloud and star formation region sight lines both display a wide range of $R_V$ values. Dust in most Galactic environments adheres to the CCM relationship, although sight lines through dark clouds and star formation regions show significant but different deviations from CCM, which may result from the presence or absence of coatings on grains (Cardelli & Clayton 1991; Mathis & Cardelli 1992). The "standard" Galactic extinction curves of Seaton (1979) and Savage & Mathis (1979) are reproduced by the CCM extinction law for one value of $R_V \sim 3.1$.

Further evidence for deviations from CCM in Galactic environments has been found by Massey, Johnson, & de Gioia-Eastwood (1995b). They have demonstrated that many Galactic OB associations have $E_{U-B}/E_{B-V}$ ratios at variance with the value of $R_V$ that would be inferred from combining optical and IR studies (e.g., NGC 6811, Hillenbrand et al. 1993; and Cyg OB2, Massey & Thompson 1991). Furthermore, the CCM relation does not fit the extinction observed in the Magellanic Clouds (e.g., Rocca-Volmerange et al. 1981; Hutchings 1982; Clayton & Martin

[1] Observer with the *Hubble Space Telescope*, which is operated by AURA, Inc., under NASA contract NAS5-26555.
[2] On leave from the Astronomical Observatory of Torino, Italy.
[3] Present address: Center for Astrophysical Sciences, The Johns Hopkins University, Department of Physics and Astronomy, 209 Bloomberg Center, Homewood Campus, 3400 N. Charles Street, Baltimore, MD 21218.
[4] NOAO is operated by the Association of Universities for Research in Astronomy, Inc., under contract with the National Science Foundation.

1985; Fitzpatrick 1985, 1986; Clayton et al. 1996). The UV (1200–3200 Å) extinction in the Magellanic Clouds displays the same general wavelength dependence as in the Galaxy, but the 2175 Å bump is weaker and the far-UV extinction is steeper (Borgman, van Duinan, & Koornneef 1975; Koornneef & Code 1981; Hutchings 1982; Nandy et al. 1980; Clayton & Martin 1985; Fitzpatrick 1985, 1986). The LMC dust in the 30 Dor region shows a weaker 2175 Å bump and steeper extinction than the Galactic CCM curve, while outside the 30 Dor region, the LMC extinction is similar to that generally observed in our Galaxy. The SMC extinction is even more extreme than the LMC 30 Dor region, with a very steep FUV rise and an almost nonexistent bump. Metallicity (heavy element abundance) differences between these three galaxies may affect the dust characteristics (Clayton & Martin 1985; Fitzpatrick 1986; Clayton et al. 1996).

Therefore, the nature of the dust extinction in M31 is of great interest because its metallicity is similar to the Galaxy (Blair & Kirshner 1985). Early work with *International Ultraviolet Explorer* (*IUE*) spectra having low signal suggested that the UV extinction observed in M31 stars had a wavelength dependence steeper than in the Galaxy (Massey, Hutchings, & Bianchi 1985; Hutchings, Massey, & Bianchi 1987; Bianchi, Hutchings, & Massey 1991). Hutchings et al. (1992) presented preliminary extinction curves of two M31 stars using *Hubble Space Telescope* (*HST*) Faint Object Spectrograph (FOS) data. These curves differ from the Galactic (CCM $R_V = 3.2$) curve by having a narrower 2175 Å bump, steep LMC (30 Dor)–like extinction in the 1450–1900 Å wavelength region, and then a turnover below 1450 Å. This FUV turnover was actually due to the preliminary FOS calibration available at that time, that caused the flux to be underestimated by up to 30%, in the short wavelengths region. Also, the previous extinction curves were obtained by comparing the observed fluxes to model atmospheres, and included both the foreground Galactic and the M31 intrinsic components. In this paper we try to separate the two components, and we mainly use the pair method to derive the extinction curves.

Massey et al. (1995a) demonstrate that $E_{U-B}/E_{B-V} = 0.5$ in M31, which is significantly different from the nominal $E_{U-B}/E_{B-V} = 0.72$ of the Milky Way. Searle (1983) found peculiar reddening in the $U$ band toward M31 globular clusters. In addition, Iye & Richter (1985) find $E_{U-B}/E_{B-V} = 1.01 \pm 0.11$ in the disk of M31 from globular cluster photometry. A study of the UV extinction curve of M31 and the comparison to Galactic and Magellanic Cloud curves can potentially answer fundamental questions about grain production and destruction.

## 2. OBSERVATIONS AND REDUCTIONS

The program star data are given in Table 1 for the foreground stars and in Table 2 for the M31 stars. Observations were made with the FOS/BL spectrograph in cycle 4 (post-COSTAR) on the *HST*. The wavelength range 1150–3300 Å was covered with gratings G160L (1150–2510 Å) plus G270H (2222–3301 Å), at a resolution of about 7 and 2 Å

TABLE 1

FOREGROUND EXTINCTION TOWARD M31

| Name | Spectral Type | $V$ | $B-V$ | $E_{B-V}$ | Angular Distance[a] (deg) | Distance[b] (pc) | References |
|---|---|---|---|---|---|---|---|
| | | | Program Stars | | | | |
| BD +41 80..... | B2 V | 9.9 | −0.13 | 0.11 | 2.1 | 2250 | 1 |
| HD 829 ..... | B2 V | 6.71 | −0.11 | 0.13 | 6.7 | 500 | 2, 3 |
| HD 6201..... | B3 V | 8.76 | −0.15 | 0.05 | 4.8 | 960 | 4, 5 |
| | | | Comparison Stars | | | | |
| HD 64802 ..... | B2 V | 5.49 | −0.20 | 0.04 | ... | ... | 6 |
| ζ Cas ..... | B2 IV | 3.68 | −0.20 | 0.04 | ... | ... | 2 |

[a] Angular separation of star from center of M31.

[b] Spectroscopic distance.

REFERENCES.—(1) Dworetsky, Whitelock, & Carnochan 1982; (2) Lesh 1968; (3) Crawford, Barnes, Golson 1971; (4) Barbier et al. 1978; (5) Balazs 1965; (6) Nicolet 1978.

TABLE 2

THE M31 PROGRAM STARS

| | FOS EXPOSURE TIMES (s) | | | | | | |
|---|---|---|---|---|---|---|---|
| NAME | G160L | G270H | $V$ | $B-V$ | $U-B$ | SPECTRAL TYPE | COMPARISON STAR |
| OB 78-159..... | 840. | 100. | 17.97: | −0.05: | −0.96: | B0 I | HD 64760 |
| OB 78-277..... | 420. | 60. | 17.35 | −0.06: | −1.15: | B1 I | HD 165024 |
| OB 78-231..... | 1920. | 180. | 18.63 | −0.19 | −1.09 | O8.5 I | HD 188209 |
| OB 48-358..... | 1750. | 180. | 18.70 | −0.06 | −0.97 | B0-1 I | HD 64760 |
| OB 48-234..... | 1080. | 140. | 18.49 | −0.02 | −0.91 | B1 I | HD 165204 |
| OB 48-444..... | 2400. | 240. | 19.10: | −0.02: | −1.04: | O8 I | HD 204172 |
| OB 8-17 ..... | 870. | 70. | 18.01: | −0.06: | −0.98: | O9–B1 I | HD 64760 |
| OB 10-64 ..... | 780. | 90. | 18.10: | −0.08: | −0.97: | B1 I | HD 150898 |

diode$^{-1}$, respectively. This is more than adequate to compare continuum distributions, and allows us to check for spectral type matches in the UV (Bianchi, Hutchings, & Massey 1996). The exposure times for each grating are listed in Table 2. Most of the data were taken in 1995 January, but the first observations of OB 78-231 failed because of technical instrument problems and were successfully repeated in 1995 July. Only this second data set is useful. The data were reprocessed, taking into account the time and focus dependence of instrument sensitivity (Lindler & Bohlin 1994; Bohlin, Lindler, & Keyes 1995), and subtracting the background estimated from the count rates below the grating cutoff (Kinney & Bohlin 1993). Three stars, OB 48-444, OB 78-231, and OB 78-277, had also been observed in cycle 1 at higher resolution using the G130H, G190H, and G270H gratings (Hutchings et al. 1992; Bianchi et al. 1994; Bianchi et al. 1996). The original FOS fluxes from the cycle 1 data for all three stars were different from the cycle 4 data by up to 32%. After we reprocessed the old cycle 1 data with the time-dependent FOS sensitivity (Lindler & Bohlin 1994), the fluxes of OB 78-231 and OB 78-277 match within 10% between the old and new data. The OB 48-444 fluxes agree well longward of 1605 Å, but the cycle 1 G130H observation still has a lower flux than the G160L data (Figure 1). The cycle 1 observations were taken through the 1″ aperture and there may have been a reacquisition problem, so that the star was not exactly centered in the aperture during the exposures with the G130H grating. The flux inaccuracy of the earlier data mainly caused the extinction curves presented by Hutchings et al. (1992) to differ from the new results presented here in the short wavelength range.

The new observations were obtained with COSTAR through the 4″.3 aperture so are less likely to have flux losses. To exclude the possibility of contamination by other stars, we chose all the program objects to be isolated, with no star of comparable brightness within a 3″ circle, to assure accurate centering in the aperture, and no UV flux contribution from other sources.

The UBV photometry and spectral types of the M31 stars given in Table 2 are from Massey, Armandroff, & Conti (1986, hereafter MAC86) and Massey et al. (1995a). The typical uncertainties in the photometry are 0.02 mag for $V = 18$ and 0.03 mag for $V = 19$ (MAC86). Photometry with colons have errors that are significantly higher than this (MAC86). Therefore, we adopt $\sigma_B = \sigma_V = 0.025$ mag for observations of stars with good photometry. Then, $\sigma_{(B-V)} = 0.035$ mag and, assuming $\sigma_{(B-V)_o} = 0.02$ mag, then $\sigma_{E_{B-V}} = 0.04$ mag. These should be considered lower limits on the errors, as they reflect internal errors rather than external errors. An important result from the optical data of Massey et al. (1995a) is that a ratio of $E_{U-B}/E_{B-V} \approx 0.5$ is required for consistent results from the photometry and spectroscopy, quite different from the Galactic typical $E_{U-B}/E_{B-V} = 0.72$. This point will be recalled in the discussion of our results.

The spectra of the M31 stars are shown in Figure 1. The recalibrated FOS cycle 1 high-resolution data are also shown with dotted lines.

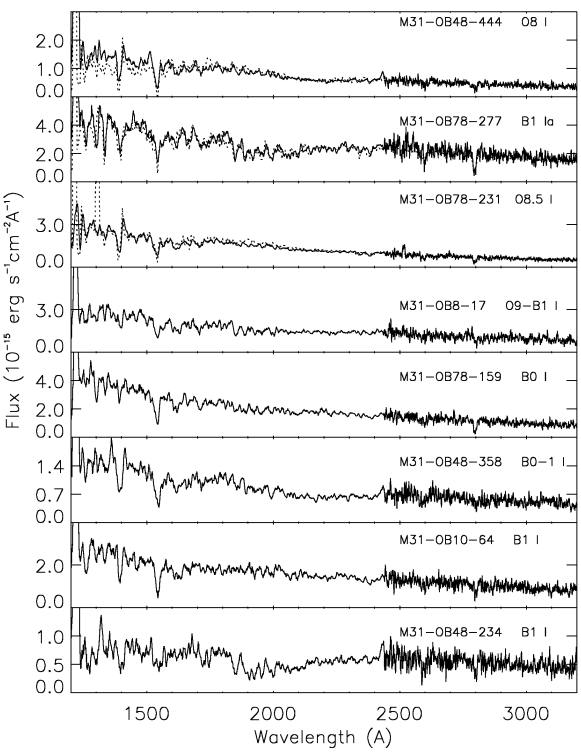


FIG. 1.—FOS spectra of the M31 program stars obtained in cycle 4. Earlier high-resolution FOS spectra for three stars are shown with dotted lines.

## 3. EXTINCTION CURVES

In this study, we construct M31 UV extinction curves by analyzing the FOS spectra with three different methods: the pair method where reddened and unreddened stars of the same spectral type in M31 are used, the pair method with comparison of M31 stars and Galactic standards, and the stellar-model-fitting method, where a model is matched to the spectrum of the reddened star by varying the temperature of the model atmosphere and the amount and type of reddening. We briefly introduce the methods below. The results will be compared in the discussion.

Virtually all UV extinction studies have used the pair method (e.g., Massa, Savage, & Fitzpatrick 1983; Witt, Bohlin, & Stecher 1984). If the spectral match between the two stars is good, then the extinction curve is well determined. The ideal application of this method to the present study is to compare pairs of stars in M31, for two reasons: (1) eliminating possible subtle spectral differences between similar stars of two different galaxies (e.g., Bianchi et al. 1996), and (2) deriving the extinction intrinsic to M31, as the foreground Galactic extinction will cancel to good approximation. This approach encounters the practical difficulty that the reddening differences between the M31 stars so far available are very small, which causes large uncertainties. The results are given in § 3.2. The sample stars are early-type supergiants, which can be used with the same accuracy as main-sequence stars in calculating extinction (Cardelli, Sembach, & Mathis 1992).

The second approach applies the pair method by comparing each of the M31 stars with an unreddened Galactic star of the same spectral type and luminosity (§ 3.3): the resulting curves have a lower fractional uncertainty, as the total reddening is larger than the intrinsic M31 reddening, but the result includes the effects of the interstellar dust in both galaxies; and assumptions have to be made to subtract the Galactic contribution. The Galactic extinction is known to vary in different lines of sight (Witt, Bohlin, & Stecher 1984). In the attempt to gain insight into the Galactic halo

extinction properties in the direction of M31, we also observed in this program Galactic objects close to the line of sight of M31 (§ 3.1).

The pair method is subject to both random and systematic errors, the largest of which is due to spectral mismatch (Massa et al. 1983). For hot stars, these errors are smaller because of their similar spectral slopes. Uncertainties in the extinction curves are estimated using the analysis of Cardelli et al. (1992) with the same assumptions, except for the higher $\sigma_{E_{B-V}}$ in our sample. Then,

$$\sigma[E(\lambda)] \sim [0.0018 + 2\sigma_V^2 + \sigma(E_{B-V})^2 2E(\lambda)^2]^{1/2}/E_{B-V}\,, \quad (1)$$

where $E(\lambda) = E(\lambda - V)/E_{B-V}$. Massa et al. (1983) derive the uncertainties in a similar way. This error estimate shows the difficulty of making accurate extinction curves for the M31 data. Assuming $E_{B-V} \sim 0.20$, then $\sigma[E(8\ \mu\mathrm{m}^{-1})] \sim 2.3$ for our program data. The difference between the Galactic CCM ($R_V = 3.2$) and LMC 30 Dor curves at 8 $\mu\mathrm{m}^{-1}$ is only 3.2.

The third method of model fitting is more complex, because a simultaneous fit must be made to the intrinsic stellar continuum and the extinction wavelength dependence. These parameters are coupled. Different combinations of stellar temperature and extinction may fit equally well the observed spectrum. However, the limitations of the data presented here prompted us to use and compare as many different methods as possible to calculate the M31 extinction.

### 3.1. *The Galactic Foreground Extinction*

The study of dust along lines of sight toward M31 is complex. These lines of sight pass through the disk and halo of the Galaxy, and then the halo and disk of M31. M31 lies at a Galactic latitude of $\sim -22°$, and the foreground extinction due to dust in the Galaxy is small: McClure & Racine (1969) found a value for the Galactic foreground extinction toward M31 of $E_{B-V} = 0.11 \pm 0.02$ mag. MAC86 find a Galactic foreground extinction of $E_{B-V} \sim 0.08$ mag. This agrees with a study of the foreground component toward Baade's Field IV ($E_{B-V} = 0.07$ mag; Humphreys 1979) and a derivation from H I measurements ($E_{B-V} = 0.08$ mag; Burstein & Heiles 1984). Hodge (1992) finds $E_{B-V} = 0.10$ mag. All of these values agree within their errors. We adopt the value for the foreground extinction of $E_{B-V} = 0.08$ mag for use in this study, because it is based on UBV photometry (also used in this paper). Scaling to the optical the extinction value determined at other wavelengths may introduce additional inconsistencies, since the ratios may differ from the Galactic canonical values, as recalled in § 1. The reddenings of our M31 objects are modest ($\leq 0.25$ mag), so it is important that the foreground component is subtracted accurately.

The Galactic foreground extinction is not known a priori along any of our lines of sight to M31. The lines of sight pass through low-density diffuse dust, which usually shows UV extinction characteristic of normal CCM $R_V = 3.1$ dust. The Galactic halo is also thought to contain this type of dust. A recent extensive UV study of halo sight lines toward Galactic stars at distances of 5–7 kpc by J. A. Cardelli (1995, private communication) shows that the halo dust extinction fits the CCM relationship in the FUV very well. However, the 2175 Å bump along these sight lines has normal strength but is narrow compared to CCM. Nothing is known about the characteristics of M31 halo dust.

Since the average total extinction of our M31 sample is $E_{B-V} = 0.20$, the absorption by the halo of our Galaxy is responsible for approximately half the total reddening; therefore, any assumption about its properties can introduce a substantial uncertainty to our conclusions. Obviously, a maximum $E_{B-V}$ of 0.08 for Galactic halo stars in the M31 line of sight is an extremely low value to derive interstellar dust properties in the UV, but we have nonetheless analyzed for this purpose spectra of some Galactic stars, lying close to the M31 line of sight and having the largest possible extinction, since it is relevant to our results. The shape of the foreground extinction curve is investigated directly for the Galactic foreground stars in Table 1. These foreground stars are all within 7° of the center of M31. The $E(B - V) = 0.05$ toward HD 6201 is too small to determine an extinction curve. Extinction curves for BD +41 80 and HD 829 are shown in Figure 2 for a 10 Å bin size.

Since the star BD +41 80 lies beyond the Galactic halo and is positioned near the edge of M31 on the sky, the top curve in Figure 2 should be the most relevant measure of the foreground extinction. However, the *HST*/FOS target acquisition was not optimal, which results in a variable loss of signal as a function of wavelength. A partial correction for this problem is made longward of 3000 Å; but a false bump still remains near $1/\lambda = 3.3\ \mu\mathrm{m}^{-1}$. The extinction curve for BD +41 80 in Figure 2 should be interpreted as an upper limit. Except for BD +41 80, *IUE* data determine other flux distributions for the other three stars used for Figure 2. The *IUE* fluxes were recalibrated to the same white dwarf flux scale as the FOS data (Bohlin et al. 1990; Bohlin 1996). The differences between the extinction for HD

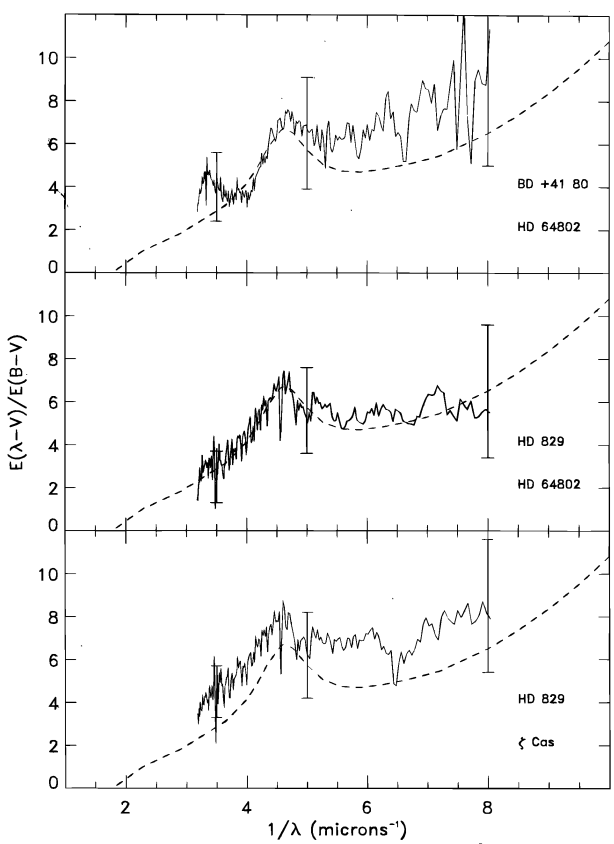


FIG. 2.—UV extinction curves obtained from Galactic halo stars within 7° of the direction toward M31. The dashed line is the Galactic extinction curve.

829 with HD 64802 as the comparison star and with ζ Cas as the comparison star are typical of the uncertainties caused by spectral mismatch. The use of Kurucz (1992) model atmosphere flux distributions for comparison stars, with the spectra of BD +41 80 and HD 829, produces extinction curves that are consistent with the top and bottom curves of Figure 2; the small amount of noise in the bright *IUE* standard star spectra is comparable to the errors in line blanketing in the models at some wavelengths.

Thus, although some of the data are suggestive of a steeper rise at short wavelengths than the typical Galactic extinction curve, the result is not conclusive, and a standard Galactic curve will be used to subtract the foreground extinction in § 3.3.

### 3.2. *Extinction from Pairs of M31 Stars*

For best results, pairs of "reddened" and "unreddened" stars both members of M31 should be used to derive extinction curves. The use of pairs of stars that are M31 members eliminates possible problems with differences between Galactic and M31 supergiants, and with uncertain Galactic foreground extinction correction.

Star pairs in M31 were chosen by using the ground-based photometry and colors (MAC86) and the spectral types from the optical spectra (Massey et al. 1995a). Comparison of OB 48-444 and OB 78-231 gives the best extinction curve, given the fairly good spectral type match and highest extinction difference. The result is shown in Figure 3. The other pairs appear to have very little extinction difference using the individual ground-based colors, and in all cases, the random uncertainty would formally be comparable to the amount of extinction.

Given the uncertainties of the *individual* photometry for our stars, we used the approach of comparing pairs of stars in different OB associations, with matching spectral types, and use the difference between the average $E_{B-V}$ of the associations to scale the extinction curve. Stars from OB 48 (average $E_{B-V} = 0.24$) are considered the reddened objects, and stars with matching spectral types in OB 78 (average $E_{B-V} = 0.12$) are used as comparisons. OB 48 is known to have considerably higher reddening than OB 78, which sits in a known H I hole (MAC86 and references therein); therefore, this approach seems the best. The resulting extinction curves appear reasonable and are shown in Figure 4. The errors are likely to be smaller than using the individual object photometry, and in fact the results from the different pairs seem fairly consistent. The feature at 2000 Å in the curve from the pair OB 48-234/OB 78-277 is caused by a Fe III line mismatch between the two stars. This has the effect of making the 2200 Å bump in the average M31 curve appear anomalously broad. The UV line spectrum of star OB 78-277 is somewhat peculiar for its spectral type, showing considerably weaker wind than Galactic stars with similar optical spectrum (Bianchi et al. 1996). In the bottom panel, the average is compared with Galactic and LMC curves. The M31 curve is similar to the Galactic extinction in the overall slope but has a lower bump at 2175 Å.

Curves obtained using the stars in the OB8 association, with the same method, are considerably worse because of strong line mismatch and therefore are not included in the average.

### 3.3. *Extinction from M31 Minus Galactic Star Pairs*

One alternative to using M31 pairs is to use unreddened Galactic supergiants as comparison stars and then subtract

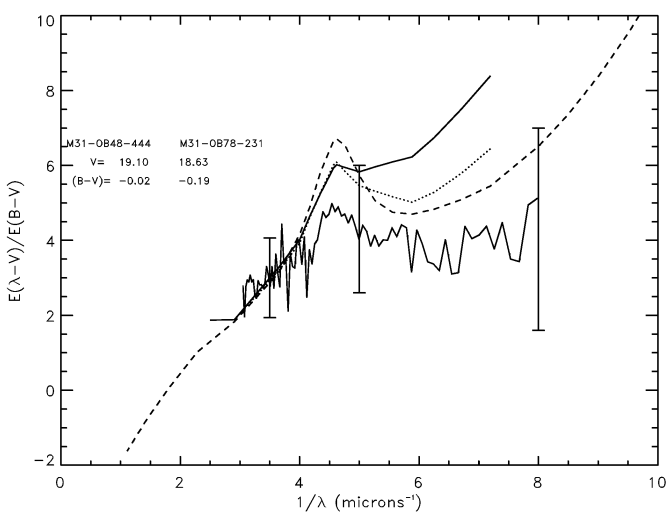


FIG. 3.—Extinction curve from one pair of M31 stars using the individual star photometry from MAC86. For comparison, the average Galactic curve (*dashed line*), the LMC (30 Dor) (*solid line*) and LMC (non–30 Dor) (*dotted line*) curves from Fitzpatrick (1985) are shown.

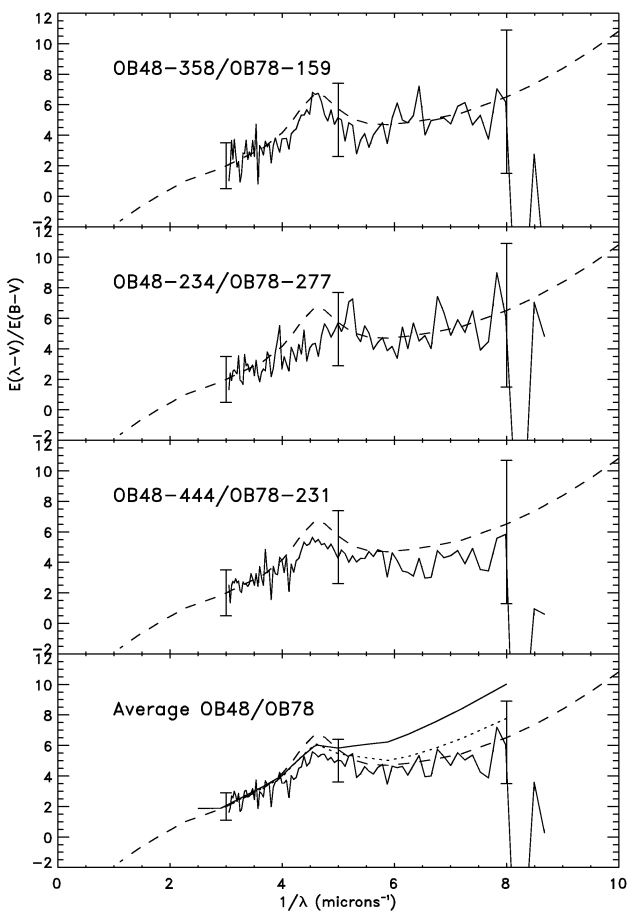


FIG. 4.—M31 UV extinction curves, obtained from pairs of M31 stars. The adopted difference in $E_{B-V} = 0.12$ is the average of the OB associations (see text). The lower panel is the average of the three individual curves above. The dashed curve is the Galactic standard extinction curve, the solid and the dotted lines are the LMC curves for 30 Dor and outside 30 Dor, respectively, as in Fig. 3.

an estimated Galactic foreground extinction. The latter method has the advantage of a much higher $\Delta E(B-V)$ for the chosen pairs but has the disadvantage of an uncertain foreground correction.

Extinction curves were calculated for all the eight M31 stars in Table 2 by comparing the FOS spectra of each M31 star to *IUE* spectra of dereddened Galactic supergiants. The comparison stars used are listed in Table 2. $E_{B-V}$ was calculated from the spectral types and the observed colors. The range of $E_{B-V}$ is 0.12–0.25 mag. Generally, reasonable extinction curves were generated, considering the large uncertainties. The curves for three stars, OB 78-277, OB 78-231, and OB 48-234, are considerably poorer than the others. These curves suffer from line mismatches and vertical shifts due to uncertainties in spectral type and photometry. The measured values of $E_{B-V}$ for the first two stars is only 0.12 mag, and the pair with OB 48-234 has a mismatch with the Fe III lines in the 2000 Å region.

The remaining five curves for OB 78-159, OB 48-358, OB 48-444, OB 8-17, and OB 10-64 were averaged, weighting each by $\sigma^2$, as calculated in equation (1). The average curve has an $E_{B-V} = 0.20$ mag. An assumed foreground component of CCM type with $R_V = 3.2$ and $E_{B-V} = 0.08$ was subtracted from the average M31 curve. Both curves, the total (M31 plus foreground) extinction, and the "intrinsic" extinction after subtracting a standard Galactic foreground, are plotted in Figure 5, with 1 $\sigma$ error bars calculated from equation (1). The M31 extinction has a 2175 Å weaker bump than the Galactic and the LMC curves shown for comparison. The extinction curves shown in Figures 4 (*bottom*) and 5 are the same within the errors, giving some confidence in the result. Both show a Galactic type FUV extinction and a weak 2175 Å bump.

From the M31 versus Galactic star pairs we also find the 2175 Å bump to be stronger generally in OB 48 stars than in the OB 78 stars. This could be due to actual differences within M31 or to a higher Galactic foreground for OB 48.

With both methods (this section and the previous one), we find the 2175 Å bump to be smaller in the M31 extinction curve than in the Galactic one, in spite of uncertainties in the Galactic foreground extinction. The difference however is only at the 1 $\sigma$ level.

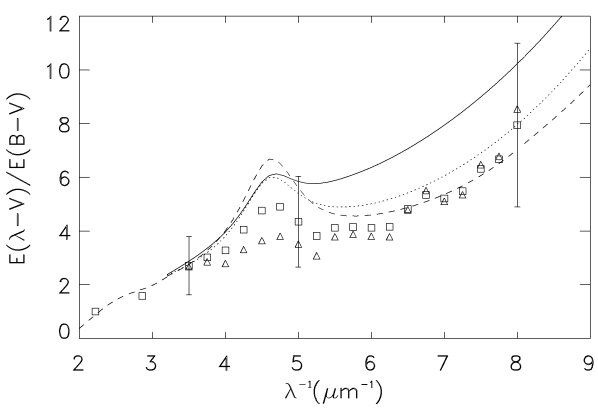


FIG. 5.—UV extinction curves from the M31 − Galactic star pair comparison. The total (Galactic + M31) extinction is plotted with squares. The extinction with a standard Galactic foreground subtracted is plotted with triangles. Also plotted are the average extinction curves for 30 Dor (*solid line*), the LMC outside of 30 Dor (*dotted line*), and the CCM law for $R_V = 3.2$ (*dashed line*). 1 $\sigma$ error bars are plotted for points at 3.5, 5, and 8 $\mu m^{-1}$.

### 3.4. *Fits to Stellar Models*

In this section we describe an approach of simple model fitting to estimate the temperatures and amounts of reddening of the program stars. This approach uses only the UV fluxes and makes no use of the ground-based estimates of spectral type and reddening. The observed FOS fluxes for the program stars were fitted with Kurucz (1992) flux models, with the application of variable amounts of Galactic (Seaton 1979) and LMC-type (30 Dor) extinction. This was initially done without reference to the star spectral types. The fits were judged subjectively, since formal fitting is complicated by several issues: the fact that two gratings were used, with different signal-to-noise ratios, differences in signal due to extinction, and regions of line blanketing not included in the stellar models. The "clean" regions to fit are the shortest wavelengths (<1400 Å), the continuum slope (>2500 Å), and the strength and shape of the 2175 Å feature. The region 1400–2000 Å, particularly the 1500–1600 Å region, is often impossible to fit. There is a large number of lines in this wavelength range that are temperature and luminosity sensitive in early-type supergiants (Cardelli et al. 1992).

The amount and shape of the extinction, and the stellar temperature, are free parameters in the fit, so that it is possible that more than one combination provide equally good fits. The fits were done "blind"—without other knowledge of the stars—and the derived temperatures and extinction were found to be similar to those derived from the ground-based photometry and the spectra. For each star a range of temperature and total extinction (in $E_{B-V}$) was noted for acceptable fits. Thus, while the mix of 30 Dor and Galactic extinction is unconstrained, the best fits usually had a range of total extinction within $\pm 0.03$, and temperature within 15%. These are comparable to and independent of the ground-based estimates of these quantities.

Using these results, we did two things. First, we compared the spectra with unreddened models of the same temperature. The ratio (or magnitude difference) shows the shape of the extinction curve, but not its absolute value. This extinction shape can be scaled to a given amount of extinction, and combined or compared for several stars. In Figure 6 we show the average total extinction scaled to $E_{B-V} = 0.1$, for the best seven stars. In deriving the mean curve, we have weighted the data by the quality of the model fits, and also excluded the poorly fit region 1500–1800 Å.

The results are quite similar for all the program stars. They measure total extinction along the line of sight, and thus contain a large fraction of Galactic halo extinction: 0.08 of the average 0.13 in $E_{B-V}$. This is true of all M31 extinction estimates that do not use pairs of stars within M31.

Second, we used the results from the model fits to select M31 pairs for comparison, relying only on the UV data. The best pairs are those with similar model temperatures and different extinction. The difference in signal between the pair stars is due to extinction and luminosity differences. This difference, expressed in stellar magnitudes, yields the shape of the extinction curve, while the zero point is determined by the intrinsic luminosity difference. Thus, the plot of the magnitude difference, scaled by the model total extinction differences, gives the *shape* of the extinction curve but with an unknown zero point. For example, if a pair has

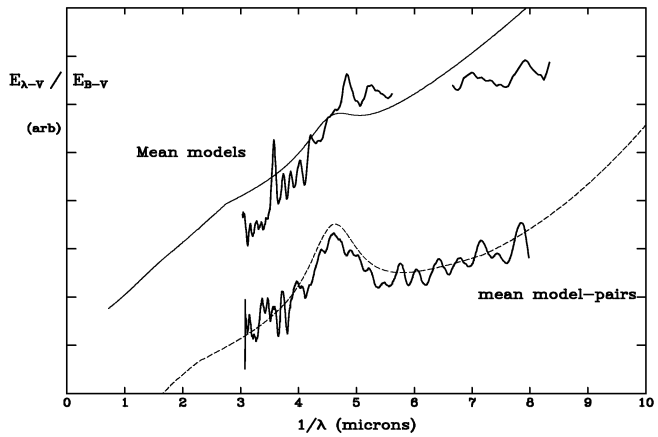


FIG. 6.—Average extinction curves from the model-fitting (*upper curve*) and model-pair (*lower curve*) methods. The upper curve is compared to the LMC 30 Dor curve. The lower curve has the average CCM ($R_V = 3.2$) curve overplotted (*dashed line*). The zero points in $E_{\lambda-V}/E_{B-V}$ are arbitrary and are separated for clarity. A region of large line mismatch has been edited from upper curve: see text for details. The upper curve includes foreground extinction. No formal error bars are plotted, since these curves are derived in a different way than those in previous figures, as described, and the arbitrary zero-point shifts imply that the scatter among the curves does not reflect absolute errors. The intrinsic M31 curve (*lower curve*) is similar to the Galactic one.

the same model temperature and a model extinction difference of 0.05, then we plotted $20 \times 2.5 \log_{10}$ (flux ratio) against $1/\lambda$. As with the model-spectra comparison, determination of the zero point was not attempted. Figure 6 also shows the mean curve from the four pairs selected in this way. The pairs used (with extinction differences from the model fits) are 444/231 ($0.12 \pm 0.03$), 358/64 ($0.08 \pm 0.02$), 358/159 ($0.05 \pm 0.03$), and 234/17 ($0.05 \pm 0.03$). The model temperatures used to select the pairs were within 1000 K for three pairs, and within 4000 K for the other. In deriving the mean curve shown in Figure 6, the pairs were weighted by the uncertainties in the extinction difference. The zero points of the two plots in Figure 6 are offset arbitrarily for clarity, and also compared with the 30 Dor and Galactic curves.

Figure 6 generally confirms the results derived by our other methods. The M31 intrinsic extinction from the pairs is similar to the Galactic one, while the total extinction, which is about 50% "foreground," is overall steeper and has a weaker 2175 Å feature.

## 4. DISCUSSION AND SUMMARY

The UV extinction curve in M31 was derived with three methods, and the following results were obtained:

1. The M31 star pairs method. Comparison of reddened and unreddened stars in M31 produces the intrinsic M31 extinction curve. The foreground Galactic extinction is eliminated, but the differences in $E_{B-V}$ for most of the pairs are very small, and thus the uncertainties are high. The results from the most reliable pairs are shown in Figures 3 and 4. The largest sources of uncertainty are the small amount of reddening and the photometric errors in the individual stars. The slope over the whole wavelength range is very similar to the "standard" Galactic curve (Savage & Mathis 1979; CCM), but the 2175 Å bump is weaker in M31.

2. The M31/Galactic pair method with reddened M31 stars and unreddened Galactic stars produced the extinction curve for the whole (Galactic + M31) line of sight. The M31 extinction curve has a weaker 2175 Å bump than the Galactic one, and a similar FUV slope.

3. Fits with stellar models also produce the total (Galactic + M31) extinction. The method has the advantage of independence from UBV photometry, but other sources of uncertainties are introduced by the model line mismatches and by the difficulty of determining both temperature and extinction at the same time. Results from the stellar model fits are also used to measure total extinction and to select and scale pairs of M31 stars. No absolute values of the extinction curve were determined by this method, but comparison of the shape with typical Galactic curves shows general agreement.

Each method has strengths and weaknesses. The pair method has the advantage of independently determining the temperature and reddening, and pairing with Galactic stars results in larger $\Delta E_{B-V}$ reducing the noise. However, the foreground is not removed, as it is using pairs of M31 stars, so a somewhat uncertain foreground correction must be made. Also, the pair method depends on the accuracy of the UBV photometry (or model fits). This becomes a large source of uncertainty, because the $E_{B-V}$ values are small. The model fit method has the advantage of not depending on the UBV photometry or spectral types, but the derived temperature and extinction are uncertain, and may not give unique solutions. Also, the stellar models do not include all line blanketing.

More highly reddened lines of sight in M31 must be observed to improve our understanding of the dust extinction properties.

Massey et al. (1995a) find that $E_{U-B}/E_{B-V}$ is lower in M31 than in either the Galaxy or the Magellanic Clouds. This low $E_{U-B}/E_{B-V}$ is not reflected in lower extinction in the near-UV (see Figs. 3–5). The results suggest that a single-parameter reddening law may be too simple to span the range of physical conditions found in regions of differing metallicity.

If the interstellar medium properties are related to galactic metal abundances, the dust in M31 should have properties more similar to the Galaxy than the Magellanic Clouds. Metal abundance values for M31 average about 0.4 dex lower than Galactic, compared with 0.7 dex for the LMC and 1.2 dex lower for the SMC (Dufour, Shields, & Talbot 1982). The average extinction curves show progressively weaker bumps and steeper FUV extinction from the Galaxy to the LMC to the SMC. A possible explanation is that the amount of dust that can be produced is limited by the abundance of condensable species. In this scenario, dust formation is self-limiting and dust forms until a large fraction of the available condensates are exhausted (e.g., Clayton et al. 1996). The results presented here for M31 do not fit this simple pattern. The M31 FUV extinction curve has a slope comparable to the Galactic standard curve, as expected for its metallicity. The weaker 2175 Å bump, if confirmed, is not typical of a high-metallicity environment. Dust extinction properties in the Galaxy vary significantly from one line of sight to another (CCM; Witt et al. 1984). Also, two distinct wavelength dependences of UV extinction have been found in the LMC, corresponding to dust inside and outside the 30 Dor region (e.g., Fitzpatrick 1986). The dust extinction

outside of 30 Dor is quite similar to Galactic CCM extinction. Thus, while grain abundances and size distributions may be primarily related to metallicity, the UV radiation present in hot star environments may have strong effects. We have no information in M31 as to whether a CCM-like relationship might exist. $R_V$ has not been measured for any of our lines of sight. Martin & Shawl (1978) found low values of the wavelength of maximum interstellar polarization for two lines of sight in M31, indicating low values of $R_V$. This parameter varies strongly from place to place in the Galaxy and in the LMC. Xu & Helou (1994) find a deficiency of very small grains in M31 from a comparison of the *IRAS* colors of Galactic and M31 cirrus. These *very small grains* may be a carrier for the 2175 Å bump feature, so an absence of such grains would lead to a weaker bump.

In summary, this study shows an indication that the extinction curve in M31 has a weaker bump than the Galactic curve (the difference however being at only 1 $\sigma$ level), but similar overall slope. This result is supported by the extinction curves derived both from M31 star pairs, and from M31-Galactic star pairs. The "model-pair" method yields only the shape of the extinction curve, and it is limited to a smaller wavelength range because of the mismatch problems, but is consistent with a CCM type curve. It will be interesting to see if there are regional differences in M31 but this is not possible with the sample used here. Future study requires lines of sight with higher reddening, and also well-matched, unreddened comparison stars in M31, to better differentiate internal and foreground dust components.

This research has made use of the SIMBAD database, operated at CDS, Strasbourg, France, and the National Space Science Data Center (NSSDC). This research was supported by grants GO-5349.02-93A (G. C. C.), GO-5349 (L. B.), NAG5-1630 (L. B.), ASI-94-RS-69 (L. B.). This work is based on observations with the NASA/ESA *Hubble Space Telescope*, obtained at the Space Telescope Science Institute, which is operated by AURA, Inc., under NASA contract NAS5-26555.

## REFERENCES

Balazs, B. 1965, Z. Astrophys., 62, 5
Barbier, R., Dossin, F., Jaschek, M., Klutz, M., Swings, J. P., & Vreux, J. M. 1978, A&A, 66, L9
Bianchi, L., Hutchings, J., & Massey, P. 1991, A&A, 249, 14
———. 1996, AJ, 111, 2303
Bianchi, L., Lamers, H., Hutchings, J. B., Massey, P., Kudritzki, R.-P., Herrero, A., & Lennon, D. 1994, A&A, 292, 213
Blair, W., & Kirshner, R. 1985, ApJ, 289, 582
Bless, R. C., & Savage, B. D. 1972, ApJ, 171, 293
Bohlin, R. C. 1996, AJ, 111, 1743
Bohlin, R. C., Harris, A. W., Holm, A. V., & Gry, C. 1990, ApJS, 73, 413
Bohlin, R. C., Lindler, D. J., & Keyes, C. D. 1995, FOS Instrument Science Report CAL/FOS-144
Borgman, J., van Duinan, R. J., & Koornneef, J. 1975, A&A, 40, 461
Burstein, D., & Heiles, C. 1984, ApJS, 54, 33
Cardelli, J. A., & Clayton, G. C. 1991, AJ, 101, 1021
Cardelli, J. A., Clayton, G. C., & Mathis, J. S. 1989, ApJ, 345, 245 (CCM)
Cardelli, J. A., Sembach, K. R., & Mathis, J. S. 1992, AJ, 104, 1916
Clayton, G. C., Green, J., Wolff, M. J., Zellner, N. E. B., Code, A. D., & Davidsen, A. F. 1996, ApJ, 460, 313
Clayton, G. C., & Hanson, M. M. 1993, AJ, 105, 1880
Clayton, G. C., & Martin, P. G. 1985, ApJ, 288, 558
Crawford, D. L., Barnes, J. V., & Golson, J. C. 1971, AJ, 76, 1058
Dufour, R. J., Shields, G. A., & Talbot, R. J. 1982, ApJ, 252, 461
Dworetsky, M. M., Whitelock, P. A., & Carnochan, D. J. 1982, MNRAS, 201, 901
Fitzpatrick, E. L. 1985, ApJ, 299, 219
———. 1986, AJ, 92, 1068
Hillenbrand, L. A., Massey, P., Strom, S. E., & Merril, K. M. 1993, AJ, 106, 1906
Hodge, P. 1992, The Andromeda Galaxy (Dordrecht: Kluwer)
Humphreys, R. 1979, ApJ, 234, 854
Hutchings, J. 1982, ApJ, 255, 70
Hutchings, J., Bianchi, L., Lamers, J., Massey, P., & Morris, S. 1992, ApJ, 400, L35
Hutchings, J., Massey, P., & Bianchi, L. 1987, ApJ, 322, L79
Iye, M., & Richter, O. G. 1985, A&A, 144, 471
Kinney, A. L., & Bohlin, R. C. 1993, STSCI-FOS Instrument Science Report CAL/FOS-103
Koornneef, J., & Code, A. D. 1981, ApJ, 247, 860
Kurucz, R. L. 1992, in The Stellar Populations of Galaxies, ed B. Barbuy & A. Renzini (Dordrecht: Kluwer), 225
Lesh, J. R. 1968, ApJS, 17, 371
Lindler, D., & Bohlin, R. C. 1994, STSCI-FOS Instrument Science Report CAL/FOS-125
Martin, P. G., & Shawl, S. J. 1982, ApJ, 253, 86
Massa, D., Savage, B. D.,& Fitzpatrick, E. L. 1983, ApJ, 266, 662
Massey, P., Armandroff, T. E., & Conti, P. S. 1986, AJ, 92, 1303 (MAC86)
Massey, P., Armandroff, T. E., Pyke, R., Patel, K., & Wilson, C. D. 1995a, AJ, 110, 2715
Massey, P., Hutchings, J. B., & Bianchi, L. 1985, AJ, 90, 2239
Massey, P., Johnson, K. E., & de Gioia-Eastwood, L. 1995b, ApJ, 454, 151
Massey, P., & Thompson, A. B. 1991, AJ, 101, 1408
Mathis, J. S., & Cardelli, J. A. 1992, ApJ, 398, 610
McClure, R. D., & Racine, R. 1969, AJ, 74, 1000
Nandy, K., Morgan, D. H., Willis, A. J., Wilson, R., Gondhalekar, P. M., & Houziaux, L. 1980, Nature, 283, 725
Nicolet, B. 1978, A&A, 34, 1
Rocca-Volmerange, B., Prevot, L., Ferlet, R., Lequeux, J., Prevot-Burnichon, M.-L. 1981, A&A, 99, L5
Savage, B. D., & Mathis, J. S. 1979, ARA&A, 17, 73
Searle, L. 1983, Carnegie Inst. of Washington Yearbook, 82, 622
Seaton, M. J. 1979, MNRAS, 187, 73
Witt, A. N., Bohlin, R. C., & Stecher, T. P. 1984, ApJ, 279, 698
Xu, C., & Helou, G. 1994, ApJ, 426, 109